J. Chem. Sci. Vol. 129, No. 11, November 2017, pp. 1735–1740.
https://doi.org/10.1007/s12039-017-1385-0

REGULAR ARTICLE

Special Issue on Recent Trends in the Design and Development of Catalysts and their Applications

Reduction of CO_2 to CO in presence of H_2 on strontium doped lanthanum manganite cathode in solid oxide electrolysis cell

NEETU KUMARI, M ALI HAIDER* and SUDDHASTAWA BASU*
Department of Chemical Engineering, Indian Institute of Technology, Delhi, New Delhi 110 016, India
E-mail: haider@iitd.ac.in; sbasu@iitd.ac.in

MS received 15 April 2017; revised 14 August 2017; accepted 24 August 2017; published online 26 October 2017

Abstract. Electrochemical performance of $La_{0.8}Sr_{0.2}MnO_{3-\delta}$ (LSM) for CO_2 reduction in solid oxide cell is studied by performing impedance spectroscopy measurement and current-voltage characterizations for varying ratio of CO_2/H_2. Ohmic resistance (R_Ω) is observed to be slightly increased from 2.59 to 2.70 $\Omega\,cm^2$, however; the cathode polarization resistance (R_2) decreased significantly from 16.20 to 4.70 $\Omega\,cm^2$ as the H_2 percentage increased from 8 to 82%, respectively. As the H_2 content increased in feed gas, the improved polarization resistance indicated an enhanced activity of LSM for CO_2 reduction reaction. Furthermore, the cathode polarization resistance for CO_2/H_2 of 92/08, is observed to be decreased from 16.20 $\Omega\,cm^2$ (OCV 0.89 V) to 1.90 $\Omega\,cm^2$ (2.0 V) as the applied potential increased in the electrolysis mode of operation. A maximum conversion of CO_2 of 6.0% with 55% of faradaic efficiency for the production of CO is achieved for CO_2/H_2 ratio of 38/62, which is supported by improved current-voltage polarization, *i.e.*, an increase in reduction current from -0.28 to -0.32 A cm^{-2} (at 2.5 V) as the CO_2/H_2 ratio decreased from 92/08 to 38/62 respectively. These results demonstrate LSM as an active electrocatalyst to reduce CO_2, which could further be improved by increasing the H_2 concentration in the feed composition to the cathode.

Keywords. CO_2 reduction; electrocatalyst; solid oxide cell; polarization resistance.

1. Introduction

In recent years, rising level of ppm concentration of CO_2 is an important concern of global warming issue.[1] Numerous ways like capture and sequestration, and chemical utilization, have been focused in literature studies to reduce the CO_2 content in the atmosphere.[2] CO_2 capture and sequestration could be an effective technique in this direction, but presently it has the issue of long time storage and handling of CO_2.[3] Chemical utilization of thermally stable CO_2 for the production of syngas mixture or hydrocarbon fuel is limited owing to an energy-intensive process.[4,5] Electrochemical reduction of CO_2 is an alternative approach to reduce CO_2 gas into hydrocarbon fuels. However, the feasibility of electrochemical reduction of CO_2 is restricted due to a high kinetic barrier of CO_2 reduction to hydrocarbon compounds.[6] Solid oxide electrolysis cell (SOEC) is a potential system to convert CO_2 into fuels and hydrocarbons.[7] Recently, significant attempts have been made to develop electrocatalytic active cathode materials to reduce CO_2 using renewable source of energy.[7–11] Ni-YSZ composites have been preferentially used as an electrocatalyst of the cathode in solid oxide cell for high-temperature electrochemical reduction of CO_2.[12] However in CO_2/CO atmosphere and at high applied potential, Ni cermet accelerates the Boudouard reaction ($2CO \rightarrow C + CO_2$) leading to carbon deposition. At this condition, the cell performance starts deteriorating.[13] Alternatively, at high temperature or reduced partial pressure of oxygen, doped ceria materials are likely to be electrocatalytically active owing to their mixed ion-electron conductive nature. Adler group have utilized Gd-doped ceria (GDC) as a cathode to perform CO_2 reduction to CO in SOEC.[14] Similarly, Cu-GDC composite cathode used to reduce CO_2 to CO with 100% faradaic efficiency.[15] Although GDC electrode is electrocatalytically active at an intermediate temperature, it shows a transition behavior towards kinetic limitation at relatively higher temperatures ($700 - 950\,^\circ C$) and lower $P_{O2} = 10^{-18} - 10^{-14}$ atm.[14] Under kinetic limitations, the entire electrode thickness is expected to be electrocatalytically inactive. Alternatively, LSM with a high electronic conductivity of 200–485 S cm^{-1}

*For correspondence

at 1000 °C,[16] has been extensively used as conventional cathode material for oxygen reduction reaction in a solid oxide fuel cell.[17] Electron conducting LSM, composited with YSZ to form a mixed conducting phase, has been utilized in a fuel cell as a stable cathode to provide a reasonably high power density.[18] In addition, recent studies have utilized LSM as an active catalyst for thermal catalytic reduction of CO_2.[19,20] Study on solar isothermal thermochemical dissociation of CO_2 has indicated LSM to be superior catalyst than ceria as it has shown higher activity for isothermal splitting (at 1400 °C) of CO_2 than that of ceria (at 1500 °C) at a relatively lower temperature.[19]

In this present work, LSM is applied as both cathode and anode to fabricate solid oxide cell with YSZ as an electrolyte. Physical characterizations are carried out to see the phase purity of electrodes on sintering at high temperature on YSZ substrate. Recent studies on CO_2 reduction on ceria surface have reported that the energy required for CO_2 adsorption followed by dissociation to CO was decreased in the presence of adsorbed hydrogen.[21–23] Therefore in this study, the cell performances are analyzed for the reduction of CO_2 by varying the CO_2/H_2 gas. The experiments are conducted to observe the CO_2 conversion and faradaic efficiencies of the cell for varying compositions of feed gas (a mixture of CO_2 and H_2).

2. Experimental

A solid oxide cell of diameter 22 mm was fabricated with an active electrode area of 0.78 cm^2. The prepared cell was comprised of yttria stabilized zirconia (YSZ) electrolyte of thickness 0.7 mm, anode and cathode each one made of lanthanum strontium manganite (LSM) of thickness 40 μm. YSZ powder (TZ-8Y, Morimura Bros., Inc., Tosoh, Japan) was mixed with 5% poly vinyl alcohol (PVA) solution and dried at 120 °C for 3 h. The dried paste was grounded to a fine powder in an electric agate mortar pastel (Ikon Instrument, Model: IK-169, India) at a speed of 120 rpm. The electrolyte pellets were prepared by pressing PVA (poly vinyl alcohol) mixed YSZ powder in a uniaxial press (Contass, Continental Scientific Syndicate, India) at 5 ton in a 25 mm diameter die and sintered at 1500 °C for 10 h with a ramp rate of 2°C/min for heating and cooling. Anode and cathode ink was prepared by mixing LSM (Sigma Aldrich) with glycerol and 20 wt.% starch (to the LSM wt.) as the pore former. A 10 mm diameter of the electrolyte was brush painted with the prepared ink and sintered at 1150 °C at a ramp rate of 1°C/min for heating and cooling.

The solid oxide cell was mounted on alumina tube using cerama bound (Lot No. 552-VFG, Aremco, NY, USA) sealant and assembled with quartz tube to allow the feed gas flow through cathode side chamber of the cell. Anode compartment of the cell was maintained at an atmospheric pressure in presence of the air. The solid oxide cell with flow system was kept inside the temperature controlled furnace and cell temperature increased to 750 °C at the ramp rate of 2°C/min. During the rise of temperature, the cathode side of the cell was exposed to pure H_2 gas at a flow rate of 60 sccm (standard cubic centimeter).

The electrochemical performance of the cell was measured using potentiostat/galvenostat (PGSTAT 128 N, Metrohom Autolab B.V., Netherland). Impedance spectroscopies were recorded in potentiostatic mode. A small alternating electrical signal of magnitude 10 mV applied across the cell and phase shifted response in the form of impedance was observed, by varying the frequency of the AC signal over several orders of magnitude from 100 kHz to 0.01 Hz to obtain the suppressed semicircular Nyquist plot. The complex impedance spectra were fitted to an equivalent RQ circuit model using ZSimpWin (Ametek, PA, USA). The high-frequency intercept on the real axis represents the electrolyte resistance or ohmic resistance (R_Ω) and the span of the arcs, denoted as the polarization resistances R_1 and R_2 corresponding to anode and cathode respectively. Linear sweep voltammetry was measured at the scan rate of 5 mV/s. Currents were measured at different applied potentials and feed gas ratio. The outlet gas was collected and analyzed by a gas chromatogram (Clarus-508, PerkinElmer, MA, USA).

X-ray Diffraction (XRD, Rigaku, MiniFlex, Japan) patterns were recorded in the range of $2\theta = 20 - 80°$, using Cu-Kα radiation with a scan rate of 4°/min and a step width of 0.02°. Scanning electron microscopy (SEM, Zeiss EVO 50) was used to analyze the fractured cross-section at the interface of electrolyte and electrodes.

3. Results and Discussion

XRD pattern of YSZ and LSM powders and sintered LSM cathode are illustrated in Figure 1. The peaks of LSM cathode compares well with the corresponding peak of YSZ and LSM powder. The SEM of the cathode-electrolyte interface, Figure 2(a), suggests LSM cathode having sufficient porosity and is perfectly adhered to the dense YSZ electrolyte. The magnified view of the cathode, Figure 2(b), illustrates well-connected sintered nanoparticles of LSM in the fabricated SOFC.

To set up the basis performance of the cell, H_2 gas is fed to cathode side and open circuit potential (OCV) is measured to be 1.11 V at 750 °C. The measured OCV value in the pure H_2 atmosphere is consistent with the theoretical Nernst potential value 1.14 V at 750 °C, suggesting no gas leakage between the two compartments of the fabricated cell. AC impedance spectroscopy of cell are recorded for the CO_2/H_2 ratio of 92/08, 74/26, 56/44, 38/62, and 18/82 at OCVs as shown in Figure 3(a). The semi-circular arc of the EIS response is fitted to an

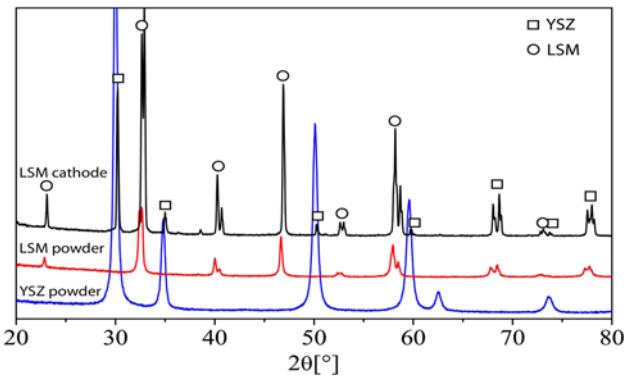

Figure 1. XRD pattern of YSZ, LSM powders and LSM cathode.

equivalent circuit (Figure 3(a)) with a pure resistor, representing the electrolyte resistance, connected in series with two analogous parallel RC circuits, each representing the response of an electrode. Pure capacitors are replaced

with constant phase element (Q_1 and Q_2) to represent the suppressed arc. The arc spanning from the high to low-frequency domain represented the total polarization resistance (R_p) offered by the two individual electrodes. The polarization resistance of anode (R_1) and cathode (R_2) were calculated from the fitted model of the impedance response. The measured ohmic (R_Ω), total polarization (R_p) and cathode polarization (R_2) resistances for varying ratio of CO_2/H_2 are summarized in Table 1. As the relative content of H_2 in feed gas increases from 8% to 82%, ohmic resistances are observed to be slightly increased from 2.59 Ω cm^2 to 2.70 Ω cm^2. Although, ohmic resistance is mainly attributed to the thick electrolyte, however the lateral interaction at the LSM-YSZ interface has a small con-

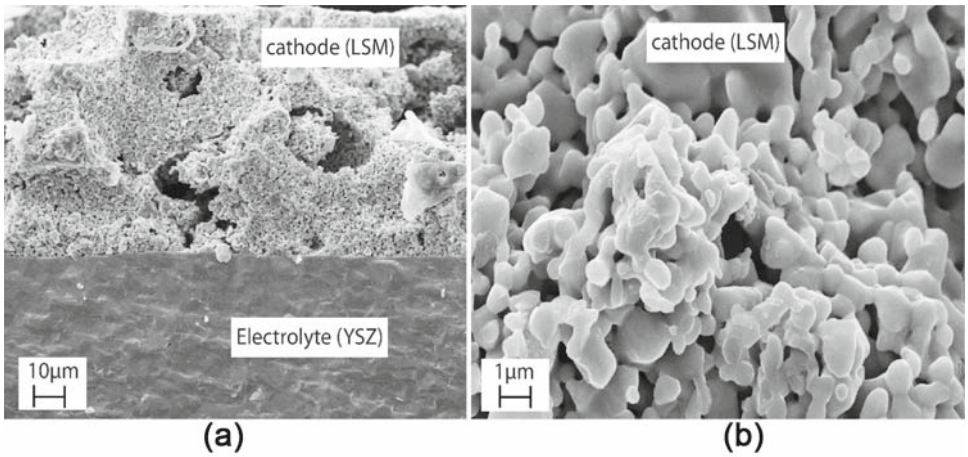

Figure 2. SEM images of the (a) electrolyte (YSZ)-cathode (LSM) interface and (b) magnified LSM cathode showing electrode morphology and microstructure.

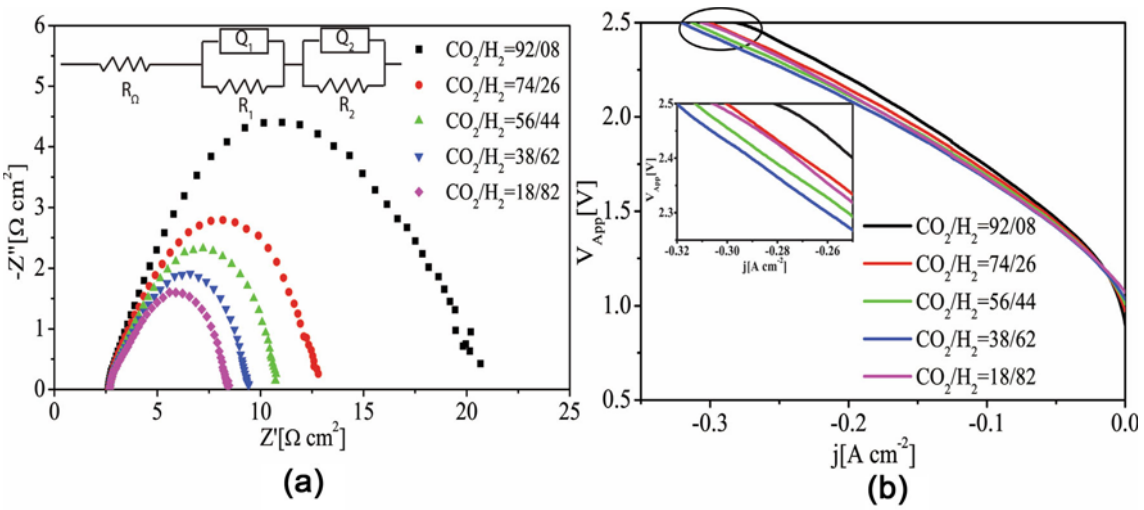

Figure 3. (a) EIS and (b) j-V characteristics of SOEC with LSM cathode, YSZ as electrolyte and LSM as an anode, in varying ratio of CO_2/H_2 at 750 °C.

Table 1. Open circuit voltage (OCV), ohmic resistance (R_Ω), total polarization resistance (R_p) and cathode polarization resistance (R_2) for varying ratio of CO_2/H_2.

CO_2/H_2	OCV [V]	R_Ω [Ω cm^2]	R_P [Ω cm^2]	R_2 [Ω cm^2]
92/08	0.89	2.59	17.20	16.20
76/24	0.96	2.65	10.40	9.40
56/44	1.00	2.68	8.20	7.20
38/62	1.03	2.69	6.79	5.79
18/82	1.06	2.70	5.70	4.70

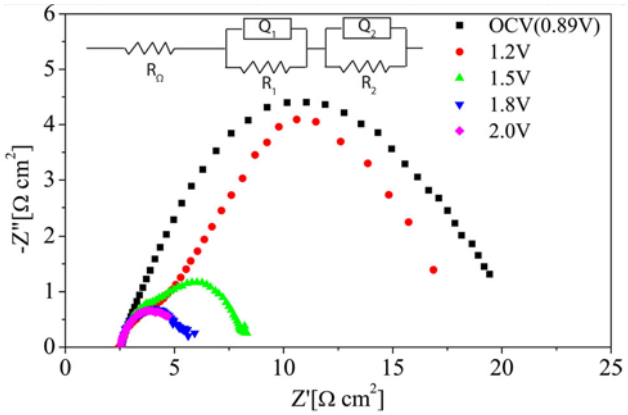

Figure 4. Impedance spectra recorded at varying applied potential in SOEC mode with LSM cathode, YSZ as electrolyte and LSM as an anode for the CO_2/H_2 ratio of 92/08 at 750°C.

tribution to R_Ω.[24] As the LSM is p-type conductor and its resistivity increases with the drop of oxygen partial pressure,[16] which may be responsible for the slight increase of R_Ω with the increase of H_2 content from 8% to 82% on the cathode side atmosphere of the solid oxide cell. On the contrary, the total polarization resistance is decreased from 17.20 to 5.70 Ω cm^2 as the CO_2/H_2 ratio decreased from 92/08 to 18/82 respectively. Similarly, the polarization resistance offered by the cathode electrode, R_2, decreased significantly from 16.20, 9.40, 7.20, 5.49 to 4.70 Ω cm^2 with the increase of H_2 concentration from 8%, 24%, 44%, 62% to 82% (Table 1), respectively. This may be due to the reduction of LSM cathode which is likely to enhance the activity for CO_2 reduction. A similar trend of polarization resistance has been observed, when CO was used as reducing gas on $(La_{0.75}Sr_{0.25})_{0.97}Cr_{0.5}Mn_{0.5}O_{3-\delta}$ (LSCM)[25] and GDC[14] based cathode materials. On LSM cathode, the total polarization resistances are observed to be of lower values (17.07 − 5.70 Ω cm^2, Table 1) as compared to the value for Cu-GDC based cathode (17.96 − 7.36 Ω cm^2) reported in an earlier study.[15]

The current-voltage (j-V) characteristics of LSM cathode measured under SOEC mode of operation for varying ratio of CO_2/H_2, are illustrated in Figure 3(b). Due to the reduction of CO_2, generated electrolysis currents are measured to the values of −0.28, −0.30, −0.31, −0.32 and −0.30 A cm^{-2} at 2.5 V for CO_2/H_2 ratio of 92/08, 76/24, 56/44, 38/62, 18/82 respectively. The inset image of Figure 3(b) clearly implies the slight improvement of negative current from -0.28 to −0.32 A cm^{-2} at 2.5 V as the relative percentage of H_2 is increased from 8% to 62%. The observation is consistent with the EIS response which suggested a significant decrease of cathode polarization resistance with the increase of H_2 percentage in the feed gas composition from 8 to 62%. In contrast to the trend, a slight decrease of reduction current from −0.32 A cm^{-2}(CO_2/H_2 = 38/62) to −0.30 A cm^{-2}(CO_2/H_2 = 18/82) at 2.5 V is observed on increasing the H_2 content from 62% to 82% (Figure 3(b)), suggesting an optimum CO_2 concentration is essential for achieving higher reaction rates.

In order to assess variation of polarization resistances with respect to varying applied potentials, the impedance spectra are recorded for the CO_2/H_2 ratio of 92/08. The ohmic and polarization resistances measured at five different potentials, OCV (0.89 V), 1.2 V, 1.5 V, 1.8 V and 2.0 V are illustrated in Figure 4 and Table 2. As the applied potential increased from OCV to 2.0 V, the measured ohmic resistance are constant to the value of 2.59 Ω cm^2, whereas, the cathode polarization resistances are improved significantly from 16.20 Ω cm^2 (OCV 0.89 V), 14.41 Ω cm^2 (1.2 V), 3.70 Ω cm^2 (1.5 V), 2.00 Ω cm^2 (1.8 V) to 1.91 Ω cm^2 (2.0 V). It is assumed that the polarization resistance reflects the impedance from the surface kinetics of CO_2 reduction reaction on the cathode. At the biased potentials in SOEC mode of operation, the LSM electrodes could become more active[17] and hence, kinetics of CO_2 electrolysis reaction commences at a relatively faster rate, resulting in a successive decrease of R_2 with an increase in biased potential. At 1.5 V of applied potential, the estimated anodic contribution of polarization resistance has become significant (1.0 Ω cm^2, Table 2) to the corresponding cathode resistance (3.70 Ω cm^2, Table 2) leading to split the total polarization curve into a bimodal arc curve (Figure 4).

Outlet gas collected from the reaction system is analyzed in the GC by using thermal conductivity detector. Inlet gas composition, operating potential, percentage conversion of CO_2, and faradaic efficiency are summarized in Table 3. Product gases are analyzed for five different compositions of inlet gas CO_2/H_2: 92/08, 76/24, 56/44, 38/62 and 18/82 at the applied potential

Table 2. Open circuit voltage (OCV), ohmic resistance (R_Ω), total polarization resistance (R_p) and cathode polarization resistance (R_2) for varying applied potentials (V_{App}) at a CO_2/H_2 ratio of 92/08.

V_{App} [V]	R_Ω [Ω cm^2]	R_P [Ω cm^2]	R_2 [Ω cm^2]	R_1[Ω cm^2]
OCV(0.89)	2.59	17.20	16.20	1.0
1.2	2.59	15.41	14.41	1.0
1.5	2.59	4.70	3.70	1.0
1.8	2.59	2.80	2.00	0.8
2.0	2.59	2.71	1.91	0.8

Table 3. Percentage conversion of CO_2, CO production rate (N'_{CO}), corresponding current density (j) and faradic efficiency (η) measured at 2.5 V of applied potential for varying CO_2/H_2.

CO_2/H_2	Applied potential (V)	CO_2 conversion (%)	N'_{CO} (ml/min)	j (A cm^{-2})	Faradic efficiency (η) %
92/08	2.5	3.1	0.35	−0.28	23
76/24	2.5	5.0	0.55	−0.30	33
56/44	2.5	5.5	0.79	−0.31	46
38/62	2.5	6.0	0.97	−0.32	55
18/82	2.5	4.7	0.83	−0.30	50

of 2.5 V. For CO_2/H_2 ratio of 92/08, percentage conversion measured to be 3.1% with a CO production rate and faradaic efficiency of 0.31 ml/min and 23% respectively (Table 3). CO_2 conversion is further improved to 5.0%, 5.5% and 6.0% as the H_2 content increases to 24%, 44%, and 62% respectively. Faradaic efficiency is enhanced to 33%, 46% and 55% as the CO_2/H_2 decreases to 76/24, 56/44, and 38/62 respectively. Similarly, the CO production rate is slightly increased from 0.55 to 0.97 ml/min with the increase of H_2 percentage from 24 to 62%, suggesting a subsequent improvement of CO_2 electrolysis performance with an increase of relative H_2 content in the feed composition. In contrast, if the H_2 percentage is further increased to 82%, the cell performance in terms of CO_2 conversion, CO production rate, and faradaic efficiency is decreased to 4.7%, 0.83, 55% respectively. The results are consistent with the j-V characteristics (Figure 3(b)) of solid oxide cell, which has indicated a subsequent increase of electrolysis current from -0.28 to -0.32 A cm^{-2} as H_2 percentage increased from 8% to 63% and then a slight decrease of current to -0.30 A cm^{-2} with further increase of H_2 to 82% (Table 3).

4. Conclusions

Solid oxide cells are fabricated with LSM as a cathode and the anode and YSZ as an electrolyte for the reduction of CO_2. Cathode polarization resistances are improved with the increase of H_2 percentage in the feed gas and it further decreases with the increase of applied potentials in the SOEC mode of operation. Current-voltage characteristic has shown a maximum reduction current of -0.32 A cm^{-2} at 2.5 V for CO_2/H_2 ratio of 38/62. CO_2 conversion up to 6% is achieved at the applied potential of 2.5 V and at a relative H_2 content of 62%.

Acknowledgements

We acknowledge the financial support of GAIL R&D, and Department of Science and Technology (DST), the Government of India. Help by Dr. Pankaj Kumar Tiwari in physical characterization of fabricated cells is acknowledged.

References

1. Dlugokencky E and Pieter T 2016 NOAA/ESRL *J. Geophys. Res.* **101** 4115
2. Yu K M K, Curcic I, Gabriel J and Tsang S C E 2008 Recent advances in CO_2 capture and utilization *ChemSusChem* **1** 893
3. Olajire A 2010 CO_2 capture and separation technologies for end-of-pipe applications—a review *Energy* **35** 2610
4. Centi G and Perathoner S 2009 Opportunities and prospects in the chemical recycling of carbon dioxide to fuels *Catal. Today* **148** 191
5. Khan M M T, Chatterjee D and Bhatt J 1992 Photofixation of carbon dioxide in semiconductor *Proc. Indian Acad. Sci. (J. Chem. Sci.)* **104** 747
6. Hori Y, Wakebe H, Tsukamoto T and Koga O 1994 Electrocatalytic process of CO selectivity in electrochemical reduction of CO_2 at metal electrodes in aqueous media *Electrochim. Acta* **39** 1833

7. Laguna-Bercero M A 2012 Recent advances in high temperature electrolysis using solid oxide fuel cells: a review *J. Power Sources* **203** 4
8. Sun X, Chen M, Jensen S H, Ebbesen S D, Graves C and Mogensen M 2012 Thermodynamic analysis of synthetic hydrocarbon fuel production in pressurized solid oxide electrolysis cells *Int. J. Hydrogen Energ.* **37** 17101
9. Xie Y, Xiao J, Liu D, Liu J and Yang C 2015 Electrolysis of carbon dioxide in a solid oxide electrolyzer with silver-gadolinium-doped ceria cathode *J. Electrochem. Soc.* **162** F397
10. Singh V, Muroyama H, Matsui T, Hashigami S, Inagaki T and Eguchi K 2015 Feasibility of alternative electrode materials for high temperature CO_2 reduction on solid oxide electrolysis cell *J. Power Sources* **293** 642
11. Li Y, Xie K, Chena S, Li H, Zhanga Y and Wu Y 2015 Efficient carbon dioxide electrolysis based on perovskite cathode enhanced with nickel nanocatalyst *Electrochim. Acta* **153** 325
12. Kim-lohsoontorn P and Bae J 2011 Electrochemical performance of solid oxide electrolysis cell electrodes under high-temperature coelectrolysis of steam and carbon dioxide *J. Power Sources* **196** 7161
13. Yue X and Irvine J T S 2012 Alternative cathode material for CO_2 reduction by high temperature solid oxide electrolysis cells *J. Electrochem. Soc.* **159** F442
14. Green R D, Liu C and Adler S B 2008 Carbon dioxide reduction on gadolinia-doped ceria cathodes *Solid State Ionics* **179** 647
15. Cheng C-Y, Kelsall G H and Kleiminger L 2013 Reduction of CO_2 to CO at Cu–ceria-gadolinia (CGO) cathode in solid oxide electrolyser *J. Appl. Electrochem.* **43** 1131
16. Jiang S P 2008 Development of lanthanum strontium manganite perovskite cathode materials of solid oxide fuel cells: a review *J. Mater. Sci.* **43** 6799
17. Jiang S P, Love J G, Zhang J P, Hoang M, Ramprakash Y, Hughes A E and Badwal S P S 1999 Electrochemical performance of LSM/zirconia–yttria interface as a function of a-site non-stoichiometry and cathodic current treatment *Solid State Ionics* **121** 1
18. Suzuki T, Awano M, Jasinski P, Petrovsky V and Anderson H U 2006 Composite (La, Sr)MnO_3-YSZ cathode for SOFC *Solid State Ionics* **177** 2071
19. Dey S and Rao C N R 2016 Splitting of CO_2 by manganite perovskites to generate CO by solar isothermal redox cycling *ACS Energy Lett.* **1** 237
20. Scheffe J R, Weibel D and Steinfeld A 2013 Lanthanum–strontium–manganese perovskites as redox materials for solar thermochemical splitting of H_2O and CO_2 *Energy Fuels* **27** 4250
21. Kumari N, Haider M A, Agarwal M, Sinha N and Basu S 2016 Role of reduced CeO_2(110) surface for CO_2 reduction to CO and methanol *J. Phys. Chem. C* **120** 16626
22. Kumari N, Sinha N, Haider, M A and Basu S 2015 CO_2 reduction to methanol on CeO_2(110) surface: a density functional theory study *Electrochim. Acta* **177** 21
23. Kumari N, Haider M A, Sinha N and Basu S 2015 Density functional theory study of CO_2 adsorption and reduction on stoichiometric and doped ceria *ECS Trans.* **68** 155
24. Cheng C Y, Kelsall G H and Kleiminger L 2013 Reduction of CO_2 to CO at Cu-ceria-gadolinia (CGO) cathode in solid oxide electrolyser *J. Appl. Electrochem.* **43** 1131
25. Yue X and Irvine J T S 2012 Impedance studies on LSCM/GDC cathode for high temperature CO_2 electrolysis *Electrochem. Solid State Lett.* **15** B31